2015

Simultaneous gas density and fuel concentration measurements in a supersonic combustor using laser induced breakdown

Hyungrok Do
University of Notre Dame

Campbell D. Carter
Wright-Patterson Air Force Base

Qili Liu
University of Notre Dame

Timothy M. Ombrello
Wright-Patterson Air Force Base

Stephen Hammack
University of Illinois at Urbana-Champaign

See next page for additional authors

Available online at www.sciencedirect.com

ScienceDirect

Proceedings of the Combustion Institute 35 (2015) 2155–2162

Proceedings of the Combustion Institute

www.elsevier.com/locate/proci

Simultaneous gas density and fuel concentration measurements in a supersonic combustor using laser induced breakdown

Hyungrok Do [a,*], Campbell D. Carter [b], Qili Liu [a], Timothy M. Ombrello [b], Stephen Hammack [c], Tonghun Lee [c], Kuang-Yu Hsu [d]

[a] *Department of Aerospace and Mechanical Engineering, University of Notre Dame, Notre Dame, IN 46556, USA*
[b] *U.S. Air Force Research Laboratory, Wright-Patterson Air Force Base, OH 45433, USA*
[c] *Department of Mechanical Science and Engineering, University of Illinois at Urbana-Champaign, Urbana, IL 61801, USA*
[d] *Innovative Scientific Solutions, Inc., Dayton, OH 45440, USA*

Available online 30 July 2014

Abstract

Laser-induced breakdown is used for quantitative gas property measurements (gas density and ethylene fuel concentration) in a cavity flameholder in a supersonic crossflow. A plasma is produced by a focused laser beam (Nd:YAG, 532 nm) in the cavity to measure gas properties at the location of the plasma and to ignite cavity flames. Plasma energy (*PE*), defined by the laser pulse energy absorbed/scattered in the plasma, and plasma emission spectra are recorded for estimating gas density and species concentration, respectively. To obtain correlations of *PE* vs. gas density and emission spectra vs. fuel concentration, calibration experiments are conducted using a variable-pressure (0–900 mbar)/temperature (300–900 K) chamber and a Hencken burner installed in a variable-pressure (50–900 mbar) combustion chamber. Total measurement time is sufficiently short, ~80 ns after laser arrival at the plasma region, to capture the high intensity portion of the emission and to minimize effects of plasma displacement (in the high-speed flow). Specifically, the laser pulse energy incident and transmitted (through the plasma) are measured, and the plasma emission spectra are captured during a 50-ns gate, after an approximate 30-ns time delay (relative to onset of emission from the plasma volume) to avoid strong background emission from the plasma.

Keywords: Scramjet; Cavity flameholder; Supersonic combustion; Laser-induced breakdown

1. Introduction

Measuring flow properties such as species concentration, pressure, temperature, and gas density in high-speed compressible flows is challenging because insertion of a physical probe can cause

* Corresponding author. Address: 109 Hessert, Notre Dame, IN 46556, USA. Fax: +1 574 631 8341.
E-mail address: hdo3@nd.edu (H. Do).

http://dx.doi.org/10.1016/j.proci.2014.07.043
1540-7489/

significant flow disturbances (e.g., shockwaves) that can alter the flow properties [1]. Therefore, optical methods have been developed and used in high-speed flows, as they provide qualitative and quantitative measurements without perturbation. In particular, spontaneous Raman scattering [2] and coherent anti-Stokes Raman spectroscopy [3] can provide species concentration and gas temperature/density. Laser-induced breakdown spectroscopy (LIBS) provides an alternate method of measuring species concentrations and gas density. It produces high emission intensity from moderate laser energy ($\geqslant$100 mJ/pulse) [4–10], and LIBS systems possess minimal system complexity. Like the aforementioned techniques, LIBS is a point measurement diagnostic; it employs a focused laser beam to generate a plasma of small volume (<1 mm^3), which acts as a virtual measurement probe [4–10]. Atomic emission line intensities of the plasma are sensitive to species concentration and are therefore used as concentration indicators in LIBS.

In a previous study [4], a nanosecond-gated LIBS (n-LIBS) method was developed to measure species concentration in a reactive flow. This newly developed n-LIBS technique minimizes measurement time required for extracting fast-decaying atomic emission lines. The minimized measurement time, <100 ns (versus >1 μs in conventional LIBS [5–10]), enables application of the LIBS technique to turbulent supersonic flows, independent of flow velocity. Otherwise, with long sampling times, the measured plasma intensity would be influenced by the flow field. Of course, high gas velocity will also act to minimize the influence of the laser-spark from one measurement to the next [4]. In this study, the pressure dependence of the n-LIBS is investigated; understanding this pressure dependence is essential for measurements in compressible flow environments. Furthermore, a new method of gas density measurement utilizing the laser-induced breakdown (d-LIB) is proposed and used in the high-speed environment. It is shown that the laser pulse energy scattered/absorbed by the plasma, defined here as the *plasma energy* (*PE*), is sensitive to gas density. A single laser shot allows both the n-LIBS and d-LIB diagnostics, enabling simultaneous measurements of fuel concentration and gas density that are used for characterizing flow properties in a cavity flameholder in a supersonic (Mach-2 freestream) wind tunnel.

2. Experimental setup

This study utilizes three facilities, a variable-temperature/pressure vacuum chamber (VTPC, Fig. 1a), a variable-pressure combustion chamber (VPCC, Fig. 1b), and a high-enthalpy supersonic wind tunnel, housed in Research Cell 19 (RC-19) at Wright–Patterson AFB. The VTPC and VPCC are for calibration purposes, providing correlations of *PE* vs. gas density and plasma atomic emission line (H/N) intensity ratio vs. equivalent fuel concentration ($X_{ethylene}$). The *PE* and H/N peak intensity ratio (PIR) are measured at various locations in and above the cavity flameholder.

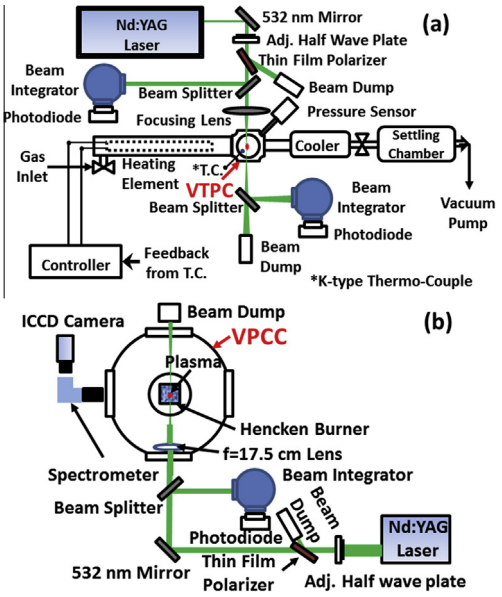

Fig. 1. Calibration experiment setups with (a) a variable-temperature/pressure chamber (VTPC), and (b) a variable pressure combustion chamber (VPCC).

Figure 1a shows the experimental setup for measuring *PE* at various pressures (*P*) and temperatures (*T*) in air within the VTPC. A small gas chamber (16 mL volume) with quartz windows for laser beam access and emission collection is connected to a resistive heating element for elevating inlet gas temperature (300–900 K). A vacuum pump pulls the gas flows (Mach number, Ma <0.1) through the chamber. A heat exchanger (cooler) and a settling chamber, placed between the chamber and the pump, serve to cool the test gas. A K-type thermocouple (2–6 K error range) and a pressure sensor (±1 mbar) are used for monitoring the test gas condition (density) in the chamber where a laser beam (532 nm, derived from an injection-seeded Quanta-Ray GCR-170 Nd:YAG laser) focused with a 175-mm focal length lens generates a plasma.

The laser pulse energy is varied using a half-wave plate mounted on an automated rotation stage and a thin-film polarizer to keep the normalized temporal/spatial laser beam profile constant. The flow field is characterized using a Pitot tube at multiple locations in the chamber at various pressures to ensure that the flow is incompressible.

Laser pulse energy traces are recorded using fast photodiodes (PD, Thor Labs): a small portion of the laser beam is split from the main beam using a fused silica window; the split beam then enters an integrating sphere. Temporal traces were then sampled and integrated in time by a digital oscilloscope (LeCroy WaveRunner 44Xi having a 400 MHz bandwidth) to derive relative beam energy; which was then put on an absolute basis by comparison to the reading from a thermopile-type power meter (Ophir).

Figure 1b shows the experimental setup for investigating the influence of pressure on X_{ethylene} measurements derived from n-LIBS. A 25-mm-square, premixed Hencken burner (premixing fuel/air upstream of the burner) is installed in the VPCC to provide flows of known species (fuel) concentrations at various pressures. The volume flow rate of ethylene (C_2H_4) and air (from *compressed air*) are controlled by electro-mechanical mass flow controllers, which are calibrated using a piston-type flow meter (Bios DryCal, Definer 220). The emission spectra from the plasma are captured by a spectrometer (Kaiser HoloSpec f/1.8) with a 100-μm-wide vertical entrance slit and an intensified CCD camera (Princeton Instrument, PI-MAX, 512 × 512 pixel array, having a Gen III intensifier tube with high quantum efficiency to 850 nm) at the spectrometer's exit plane. A Nikon camera lens (58 mm, f/1.2) is used to collect plasma emission and focus it on the entrance slit. Tuning of the spectrometer is accomplished by translating the CCD camera along the exit plane, and a range from 550 to 700 nm is acquired (approximately 0.3 nm/pixel). The plasma emission spectra are collected during a 50-ns gate time approximately 30 ns (<5 ns jitter) after initial emission from the plasma region (that appears a few ns after the arrival of a laser pulse).

The plasma is placed at multiple locations (34 total, see Fig. 2) in and above a cavity flameholder of the RC-19 wind tunnel. The cavity flame is ignited by the plasma when placed below the red dotted curve (Fig. 2) in the cavity. The width of the combustor is 152 mm, and a cavity flameholder (depth of 16.5 mm, length of 66 mm, to the ramp midpoint, and closeout ramp angle of 22.5°) is located on the bottom wall of the wind tunnel; this bottom wall diverges (from the horizontal plane) at an angle of 2.5°. The wind tunnel has fused silica windows on both side walls and the top wall. A

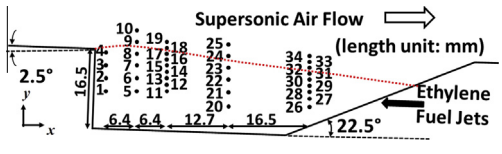

Fig. 2. Locations of the plasma in and above the cavity flame holder.

focusing lens of 175-mm focal length is placed approximately 75 mm from the outer surface of the window so that the plasma is at the center (symmetry) plane of the tunnel. While the laser pulse energy could be adjusted with rotation of the half-wave plate, this rotation was somewhat slow. Thus, for the wind tunnel measurements, the Q-switch delay was changed to initiate or inhibit breakdown. Normally, there was some delay (~1 s) associated with this process of achieving optimum lasing energy. Of course, this delay was quantified with the measurement of the incident pulse energy.

The measurement locations (see Fig. 2) L1–L10 and L20–L25 are vertically (y-direction) aligned with 2.5-mm separation; L11–L19 and L26–L34 are also vertically aligned and spaced 1.25 mm apart. The vertical lines of the plasma locations are spread horizontally (x-direction) to cover the primary recirculation zone of the cavity. Location 1 (L1), the origin of a reference x–y coordinate, is ~7.6 mm above the cavity bottom and 2.5 mm from the cavity front step. The laser beam is slightly inclined vertically (~4°) in order to block side-window reflected beam (using a beam aperture located between the focusing lens and the side window) and avoid damage to optics. The HoloSpec spectrometer collects the emission from the plasma through the top window during a 50-ns gate time ~30 ns (<5 ns jitter) after initial plasma emission as in the calibration experiments. Note that the plasma moves at most 60 μm during measurements (80 ns) in RC-19, given the Ma-2 freestream conditions (~750 m/s at 600 K stagnation temperature). Simultaneously, the incident and transmitted laser pulse energies were recorded using the photodiodes and oscilloscope. All of the optics, the spectrometer, and the laser are on an optical table driven by a 3-axis automated translation stage that is used to position the plasma within the wind tunnel flow field. Static pressure distribution in the cavity flameholder is measured by pressure transducers on the front step, cavity floor, and ramp surfaces.

3. Results

3.1. Gas density measurement (d-LIB)

Gas density significantly affects the laser-induced breakdown phenomena because it determines the number of molecules absorbing and scattering laser energy in the plasma volume and thus the net laser beam extinction [4]. To establish a universal correlation of PE vs. T/P applicable to wide ranges of T and P, both are varied in the VTPC from $T = 300$ to 900 K, and from $P = 100$ to 850 (±5) mbar. As shown in Fig. 3, it is confirmed that the PE measured with the various T and P are on a single curve providing a

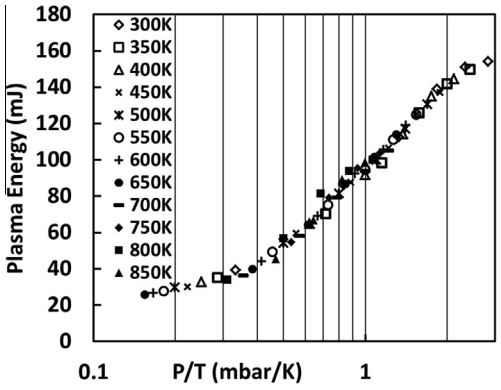

Fig. 3. PE vs. P/T in VTPC.

one-to-one function that allows direct PE to P/T conversion.

Possible error sources in measuring PE are identified, which are fluctuations in the incident laser pulse energy (E_0, measured before the plasma), laser beam reflection/absorption by windows, and dependence of PE on species (fuel) concentration. The influence of the changes or fluctuations in E_0 on PE is quantified in the same ranges of P and T with varied E_0 (165–340 mJ) to establish a universal function deriving gas density (P/T) from PE and E_0. In the calibration experiments, E_0 fluctuation with the injection-seeded Nd:YAG laser is typically within ±2% around the mean, and the corresponding PE fluctuation amplitude is at most within ±5%. Considering that PE linearly increases with E_0 in the ranges of $E_0 = 165$–340 mJ and $P/T = 0.1$–3 mbar/K, the measurement uncertainty range can be reduced to ±3% utilizing the universal function and instantaneous PE/E_0 measurements. In addition, the laser pulse energy reflected or absorbed by optical access windows is measured with various E_0 to correct the tunnel measurements. Finally, because the calibration experiments are conducted in air, the weak dependence of PE on species concentration [4] is considered for the d-LIB measurements in the cavity flameholder, where mixtures of ethylene/air/combustion products are found (see Section 3.3).

3.2. Ethylene fuel concentration measurement

Plasma emission spectra (550–700 nm) in reactants and combustion products are recorded in the VPCC at various pressures. N (568 nm) and H (656 nm) atomic emission-line peak intensities are measured to correlate the H/N peak intensity ratio (PIR) with H/N atom number ratio or *equivalent* ethylene *concentration*, X_{ethylene}.

$$\frac{\text{H}}{\text{N}}_{\text{atom ratio}} = \frac{2.5 \times X_{\text{ethylene}}}{(1 - X_{\text{ethylene}})}$$

It is noted that X_{ethylene} is used consistently throughout this paper, for both reactants and product streams. Calibration curves of H/N PIR vs. X_{ethylene} are obtained in a range from $P = 470$ to 800 mbar that covers typical RC-19 tunnel test conditions. Flow unsteadiness, leading to transient beam steering effects and decreased signal-to-noise ratio within the products, are possible measurement uncertainty sources.

Figure 4 presents emission spectra (average of 100 instantaneous spectra) from the plasma in reactants (Fig. 4a) and products (Fig. 4b) at various P. In reactants, the H/N PIR (H peak intensity normalized by N peak intensity) decreases markedly with increasing P at a constant H/N atom number ratio (19.5% ethylene mole fraction), while the PIR in products is nearly insensitive to P. Ideally, the H/N PIR would be independent of P and T prior to the laser-induced breakdown because P and T in the plasma are extremely high (estimated at 50–175 bar and 15,000–50,000 K [11,12], respectively). Nevertheless, the effect of P on the H/N PIR is obvious in reactants as shown in Fig. 4a. We conjecture that this pressure effect involves emission-line self-absorption [13] and interactions of the excited/dissociated species in the plasma with the surrounding gas medium (e.g., chemical reactions including radical/ion recombination and energy transfer/relaxation during the measurement time). The dissociated radical species are highly excited and capable of initiating reac-

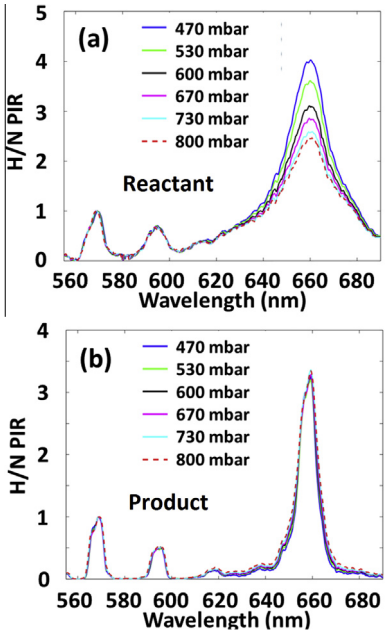

Fig. 4. Emission spectra recorded in (a) reactant gas ($X_{\text{ethylene}} = 19.5\%$) and (b) in combustion product gas ($X_{\text{ethylene}} = 10.4\%$). The spectra are normalized by nitrogen peak intensity at 568 nm.

tions, particularly in gases having reactive species (fuel/oxidizer) and relatively high number density. Interactions of the plasma within the products, on the other hand, are less significant.

The calibration curves of ethylene concentration (mole%) vs. H/N PIR at various P are plotted in Fig. 5. The different trends in Fig. 5a and b would be from altered plasma characteristics under the distinctive gas conditions in reactants and products [4]. The experimental calibration data are obtained in two ranges of ethylene concentration, 3–35% (equivalence ratio $\phi = 0.45$–7.3) in reactants (plasma at 3 mm above the burner) and 4.5–12% ($\phi = 0.67$–2.0) in products (plasma at 10 mm above the burner). These ranges are limited by accessible flow conditions in the VPCC for (i) generating flows fast enough to induce flame blow-off for measurements in reactants, and (ii) sustaining stable flames on the Hencken burner to provide stable product gas flows for measurements in the products. In reactants, the effect of P is more pronounced at higher X_{ethylene}, as shown in Fig. 5a, while the effect of P is unremarkable in products throughout the whole measurement range (Fig. 5b). It is noteworthy that the combustion products of fuel-rich flames ($\phi > 1$) contain residual fuel that is not in the products of fuel-lean flames ($\phi < 1$). This implies that, at least under the high-T conditions in products within the range of $\phi = 0.67$–2.0, the H/N PIR primarily depends on H/N atom number ratio, which is not affected by the origin of H atoms (e.g., ethylene fuel, combustion intermediate species or major product species such as water).

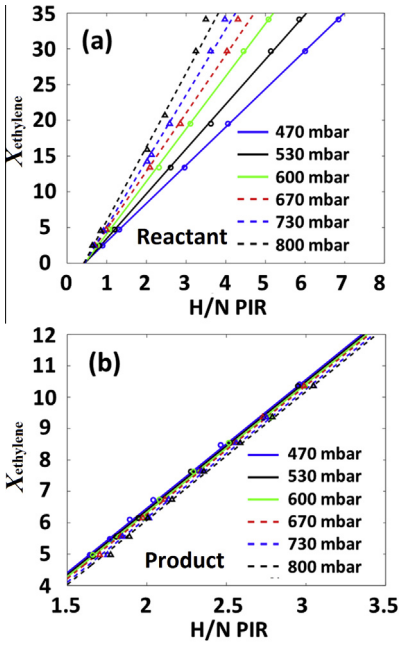

Fig. 5. X_{ethylene} (%) vs. H/N PIR under various pressure conditions, 470–800 mbar: (a) in reactants, and (b) in combustion products.

3.3. Gas density and equivalent ethylene concentration measurements in RC-19

Cavity flames are ignited by the laser-induced plasma at various locations, enabling measurements of gas density and equivalent ethylene concentration in the RC-19 supersonic wind tunnel using the correlations obtained in the calibration experiments. The freestream Ma, stagnation pressure and stagnation temperature are 2, 4.74 bar and 600 K, respectively. Multiple subsonic ethylene injectors are located on the cavity ramp, injecting fuel toward the front step as indicated in Fig. 2. The fuel injection rate is fixed at 56 standard liters/min (SLPM, corresponding to 273 K and 1.013 bar conditions). The plasma generated for gas property measurements by the focused laser beam is also used as an ignition source. The cavity flame is not ignited when the plasma is placed above the cavity shear layer. The boundary of the ignitable region is delineated in Fig. 2 (red dotted curve). The flow field was not characterized or visualized for this experiment, but the shear layer is presumably adjacent to the boundary of the ignitable area. A total of 300 laser pulses are generated at locations L1–L34 with 10-Hz repetition frequency, while the laser pulses for the first few seconds (a few tens of laser pulses) are at low energy due to the "detuned" Q-switch delay. Sample results are provided in Fig. 6.

At most of the locations below the shear layer, the cavity flame is ignited within several high-energy laser pulses. Nevertheless, the flame ignition is delayed near the fuel jet and the shear layer where fuel and oxidizer are not well mixed and/or the stretch rate is relatively high; this is illustrated in the 4 plots of Fig. 6 that shown X_{ethylene} with the

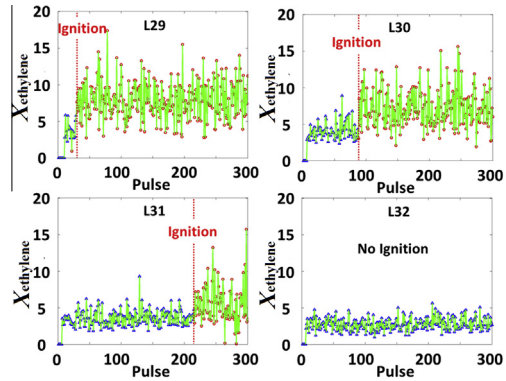

Fig. 6. X_{ethylene} measurements on a vertical line (L29 through L31) across the shear layer.

300 laser pulses at each location. L32 is right above the ignition boundary, and L31 through L29 are aligned vertically downward with 2.5-mm spacing. The red dotted vertical lines in the plots indicate the laser pulse at which cavity ignition is achieved. The presence of a cavity flame can be determined easily (after ignition) by the decrease in backgro und plasma emission (Fig. 7), due to the increase in temperature and concomitant decrease in gas density. When this occurs, the calibration curve is switched from that for reactants to that for products. Prior to ignition, it is expected that the measurement error increases near/above the shear layer due to non-uniform, unsteady pressure fluctuations. The delay of cavity flame ignition increases as the plasma location approaches the ignition boundary or shear layer: 2 s delay at L29, 8 s at L30, and 20 s at L31. Before the cavity flame ignition, the X_{ethylene} on the vertical line (L29–L32) does not vary (3–6%) significantly, while it slowly decreases as the plasma location moves upward toward the freestream. The average X_{ethylene} (~4.5%) is marginal (near the lean flammability limit) to initiate combustion, and therefore the probability of flame ignition in this region by a single plasma pulse is relatively low. It is noteworthy that multiple plasma pulses would not benefit ignition due to the low pulse repetition rate (10 Hz) in the high-speed environment that prohibits accumulation of radicals from preceding plasma pulses in the cavity. However, the increase of X_{ethylene} and reduction of stretch rate below the shear layer will obviously increase the probability of ignition (or reduce the delay of cavity ignition) as shown in Fig. 6. This gradual change in X_{ethylene} along the vertical line (L26–L34) makes the boundary of the ignitable region unclear near the cavity ramp.

On the other hand, the boundary of the ignitable region is clear at locations closer to the front step of the cavity where the shear layer is thin. Figure 8 presents X_{ethylene} along the vertical line of L5–L10. It is noteworthy that the first plasma pulse has ignited the cavity flame at L5 through L7 where X_{ethylene} before ignition is in a range of 6–8% or $\phi = 0.9$–1.4. Interestingly, once the cavity flame is ignited, the estimated X_{ethylene} at the location increases up to 9–12% or $\phi = 1.4$–2, which is due, presumably, to alteration of the flow field (lifting of the shear layer, leading to reduced air entrainment into the cavity) by the combustion heat release. Presumably too, the locations of L5–L7 are in the primary recirculation zone where fuel and air are relatively well mixed and the gas is at low speed and thus ideal for locating an ignition source. Otherwise, ignition is delayed (~10 s or 100 laser pulses) at L8, which is just below the ignition boundary. We conjecture that the stretch rate at L8 would be relatively high because the shear layer is thin with a steep velocity gradient along the vertical line. Also, the steep X_{ethylene} gradient between L8 (5–10%) and L9 (0.4–0.6%), as shown in Fig. 8, would lower the probability of ignition at L8 and limit the growth of plasma-induced flame kernel. The plasma locations L9 and L10, having negligible fuel concentrations, are above the shear layer; the H line emission detected at these locations would be from water contained in the freestream (since the wind tunnel takes in ambient air).

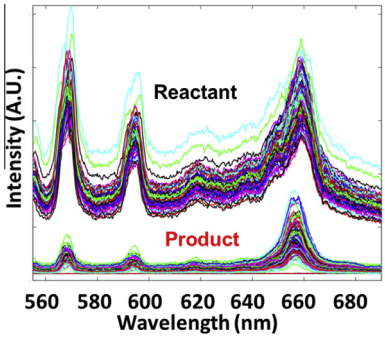

Fig. 7. Un-processed raw spectra captured at L30.

Based on the point measurements at the 34 plasma locations after cavity ignition (and linear interpolation between the locations), time-averaged, 2-D X_{ethylene} and T distributions are derived and illustrated in Fig. 9. In practice, the cavity with a flame is filled with a mixture of combustion products, entrained air, and fresh fuel. However, the n-LIBS provides only equivalent ethylene fuel concentration (X_{ethylene}) in air as discussed above; preferential diffusion effects, combustion efficiency or intermediate reaction progress of the mixture cannot be estimated by the measurement employing H/N PIR as the fuel concentration indicator. T after ignition is derived from the P/T measurement assuming a uniform pressure distribution in the region of interest (below the shear layer). T in the presence of fuel is slightly underestimated by as much as 50 K with the ethylene concentration range below 12% due to the increased PE [4]. In spite of these challenges associated with the measurement technique, the 2-D fields obtained here provide useful global information of the important cavity flow parameters. For example, as observed in Figs. 6 and 8, the X_{ethylene} gradient in the y-direction across the shear layer becomes gradual as the flow approaches the ramp, which is due to the growth of the cavity shear/mixing layer. In addition, a relatively high and uniform X_{ethylene} region (red area in Fig. 9a) below the shear layer is observed that represents the primary cavity recirculation zone. In addition, the T distribution (Fig. 9b) in the cavity indicates existence of a hot pocket near the front step and a high-T region, probably a flame zone or region with a moderately high concentration of products, right

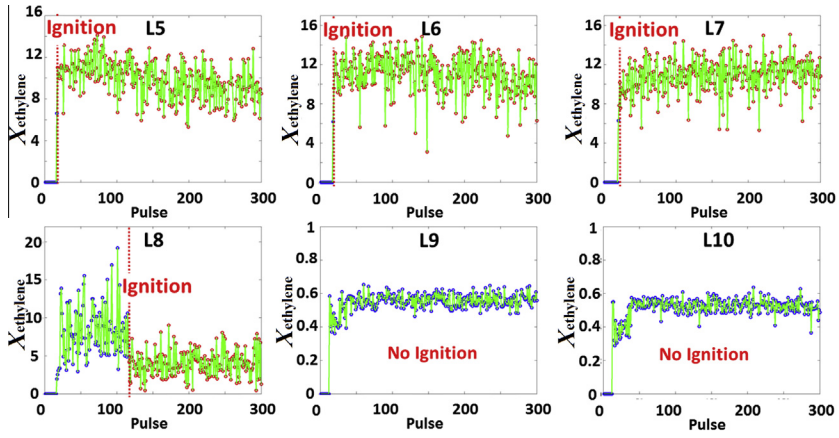

Fig. 8. $X_{ethylene}$ (%) on the vertical line L5–L10.

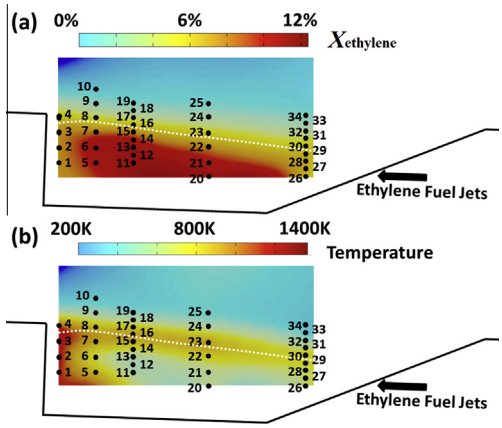

Fig. 9. 2-D (a) $X_{ethylene}$ and (b) temperature fields after the cavity flame ignition.

below the shear layer. Interestingly, the high-T region is coincident with a stoichiometric mixture line ($X_{ethylene} = 6.5\%$ or $\phi = 1$) in Fig. 9a (white dotted curve). This is because a strong combustion zone resides along the stoichiometric mixture line below the shear layer, which was confirmed in a previous study with the same cavity configuration and similar ethylene fuel flow rate (59.8 SLPM) [14]. In that study, the presence of OH showed that a strong flame zone lies along the cavity-flameholder shear layer.

4. Summary

Fuel concentration and gas density were measured simultaneously in a cavity flameholder of a supersonic wind tunnel using laser-induced breakdown (LIB). Both properties were measured within 80 ns after each laser pulse to minimize the measurement uncertainty in high-speed flows. The plasma discharge induced by a focused laser beam served as the measurement probe as well as the cavity flame igniter when placed below the cavity shear layer where fuel and entrained air are relatively well mixed. Flame ignition in the cavity can be conveniently detected by the sudden decrease in plasma emission intensity and the plasma energy (or *PE*, defined as the laser energy absorbed/scattered in the plasma) due to the decreased gas density in high-temperature combustion products. The so-called equivalent fuel concentration ($X_{ethylene}$, ethylene concentration prior to burning) and gas density after combustion ignition were simultaneously measured at 34 locations, mostly within the cavity. The 2-D fields of $X_{ethylene}$ and temperature depicted the existence of a (i) hot pocket near the front step of the cavity that also possesses a uniform, high $X_{ethylene}$, and a (ii) strong combustion or high-temperature zone below the shear layer (i.e., on the cavity side) that is coincident with a stoichiometric mixture line.

These measurements in the compressible, subatmospheric pressure (<1 bar), high-speed environment were enabled by experiments conducted in a variable-pressure/temperature chamber (VPTC) and a variable-pressure combustion chamber (VPCC) to provide calibration curves correlating *PE* vs. gas density and H/N atomic-line peak intensity ratio (PIR) vs. $X_{ethylene}$. The *PE*, based on the difference between transmitted and incident laser energy, was recorded over a wide range of static pressures (100–850 mbar) and temperatures (300–850 K) in the VPTC to confirm that the *PE* can serve as a gas density indicator under the typical test conditions found within the cavity flameholder. In addition, it was shown that the H/N PIR in high-temperature combustion products is not sensitive to static pressure and temperature, while pressure changes in reactants significantly affect the PIR under a

constant $X_{ethylene}$ conditions. We conjecture that this is due to the self-absorption of the H emission line in relatively high-density reactants and the interactions between the surrounding reactants and the excited species in the plasma.

Acknowledgement

This work is supported by the American Society for Engineering Education (ASEE, through the Summer Faculty Fellowship Program), the Air Force Research Laboratory (AFRL), and the Air Force Office of Scientific Research (AFOSR FA9550-12-1-0161, Program Officer: Dr. Chiping Li).

References

[1] S. Tavoularis, *Measurement in Fluid Mechanics*, Cambridge University Press, New York, USA, 2005, p. 193.
[2] R.W. Pitz, N.R. Grady, S.W. Shopoff, S. Hu, C.D. Carter, *UV Raman Scattering Measurements of a Mach 2 Reacting Flow over a Piloted Cavity*, 46th AIAA Aerospace Sciences Meeting and Exhibit, Reno, Nevada, 2008, AIAA 2008–244.
[3] A. Cutler, G. Magnotti, L. Cantu, E. Gallo, P.M. Danehy, R. Rockwell, C. Goyne, J. McDaniel, *Dual-Pump CARS Measurements in the University of Virginia's Dual-Mode Scramjet: Configuration "C"*, 51st AIAA Aerospace Sciences Meeting including the New Horizons Forum and Aerospace Exposition, Grapevine, TX, 2013, AIAA 2013–0335.
[4] H. Do, C.D. Carter, *Combust. Flame* 160 (2013) 601–609.
[5] V. Strum, R. Noll, *Appl. Opt.* 42 (2003) 6221–6225.
[6] B.C. Windom, P.K. Diwakar, D.W. Hahn, *Spectrochim. Acta, Part B* 61 (2006) 788–796.
[7] L.G. Blevins, C.R. Shaddix, S.M. Sickafoose, P.M. Walsh, *Appl. Opt.* 42 (2003) 6107–6118.
[8] F. Ferioli, P.V. Puzinauskas, S.G. Buckley, *Appl. Spectrosc.* 57 (2003) 1183–1189.
[9] F. Ferioli, S.G. Buckley, *Combust. Flame* 144 (2006) 435–447.
[10] S.H. Lee, H.T. Hahn, J.J. Yoh, *Spectrochim. Acta, Part B* 88 (2013) 63–68.
[11] Ş. Yalçin, D.R. Crosley, G.P. Smith, G.W. Faris, *Appl. Phys. B* 68 (1999) 121–130.
[12] N. Glumac, G. Elliott, M. Boguszko, *AIAA J.* 43 (9) (2005) 1984–1994.
[13] C. Aragon, J. Bengoechea, J.A. Aguilera, *Spectrochim. Acta, Part B* 56 (2001) 619–628.
[14] K.-Y. Hsu, C.D. Carter, M.R. Gruber, T. Barhorst, S. Smith, *J. Propul. Power* 26 (2010) 1237–1246.